3D molecular line formation in dwarf carbon-enhanced metal-poor stars

N. T. Behara[1,2], H.-G. Ludwig[1,2], P. Bonifacio[1,2,3], L. Sbordone[1,2], J. I. Gonzalez Hernandez[1,2], & E. Caffau[2]

Galaxies Étoiles Physique et Instrumentation

[1]CIFIST Marie Curie Excellence Team
[2]GEPI, Observatoire de Paris-Meudon, France
[3]INAF, OA Trieste, Italy
natalie.behara@obspm.fr

Abstract

We present a detailed analysis of the carbon and nitrogen abundances of two dwarf carbon-enhanced metal-poor (CEMP) stars: SDSS J1349-0229 and SDSS J0912+0216. We also report the oxygen abundance of SDSS J1349-0229. These stars are metal-poor, with [Fe/H] $<$ –2.50, and were selected from our ongoing survey of extremely metal-poor dwarf candidates from the SDSS.

The carbon, nitrogen and oxygen abundances rely on molecular lines which form in the outer layers of the stellar atmosphere. It is known that convection in metal-poor stars induces very low temperatures which are not predicted by 'classical' 1D stellar atmospheres. To obtain the correct temperature structure, one needs full 3D hydrodynamical models. Using CO^{5}BOLD 3D hydrodynamical model atmospheres and the Linfor3D line formation code, molecular lines of CH, NH, OH and C_2 were computed. 3D carbon and nitrogen abundances were determined, and the resulting carbon abundances were compared to abundances derived using atomic C I lines in 1D LTE and NLTE. For one star we were able to compare the 3D oxygen abundance from OH lines to O I lines in 1D LTE and NLTE.

There is not a good agreement between the carbon abundances determined from C_2 bands and from the CH band, and molecular lines do not agree with the atomic C I lines. Although this may be partly due to uncertainties in the transition probabilities of the molecular bands it certainly has to do with the temperature structure of the outer layers of the adopted model atmosphere. In fact the discrepancy between C_2 and CH is in opposite directions when using 3D and 1D models. Confronted with this inconsistency, we explore the influence of the 3D model properties on the molecular abundance determination. In particular, the choice of the number of opacity bins used in the model calculations and its subsequent effects on the temperature structure and molecular line formation is discussed.

Introduction

SDSS J1349-0229 and J0912+0216 were selected from our ongoing survey of extremely metal-poor star candidates from the Sloan Digital Sky Survey. SDSS J1349-0229 has an effective temperature of 6200 K, log g = 4.00 and [Fe/H] = –3.00. SDSS J0912+0216 is slightly hotter with a temperature of 6500 K, log g = 4.50 and [Fe/H] = –2.5. These two stars belong to the class CEMP-r/s, since their atmospheres are enhanced in carbon, and show overabundances in s and r-process elements. For details regarding the abundances of the neutron capture elements, refer to Behara et al. (2009), as well as a poster presented in Symposium 265 by the same authors.

The focus of this study is on the abundances of CEMP stars determined predominately using molecular lines: carbon, nitrogen and oxygen. It is known that overcooling in the outermost layers of metal-poor stars produced by convection is not predicted by classical 1D stellar atmospheres and is best reproduced by 3D hydrodynamical simulations (Asplund et al. 1999; Caffau & Ludwig 2007; González Hernández et al. 2008). An accurate description of these outer layers is crucial for the determination of the molecular abundances.

We are fortunate that these two CEMP stars are hot enough to display atomic carbon lines. These lines are formed much deeper in the atmosphere compared to the molecular lines, and are thus shielded from the overcooled region of the atmosphere, allowing for a validity check of the abundances obtained from the molecular lines.

Abundance analysis

In our analysis, we used 3D model atmospheres computed with the CO^{5}BOLD code (Freytag et al. 2002; Wedemeyer et al. 2004). The 3D spectral synthesis calculations were performed with the code Linfor3D. The parameters of the 3D models used are listed in Table 1.

We compared each of our 3D models to a corresponding standard hydrostatic 1D model, and define the 3D correction of an abundance measure in the sense 3D – 1D. The 1D models are calculated using plane-parallel geometry and employ the same equation-of-state and opacities as the CO^{5}BOLD models.

With the exception of C_2, all of the abundances were determined using equivalent widths of unblended lines. The C_2 abundance was determined using line fitting. For CH, we adopted the line list used by Bonifacio et al. (1998), for the UV OH lines the gf values have been computed from the lifetimes calculated by Goldman & Gillis (1981), and for C_2 and NH we used the molecular line lists by Kurucz (2005). The results for the two stars are listed in Table 2.

Model	T_{eff}	log g	[Fe/H]	#OB
d3t63g40mm30n01[a]	6270	4.00	–3.0	6
d3t65g45mm20n01[b]	6530	4.50	–2.0	6
d3t65g45mm30n01[b]	6550	4.50	–3.0	6
d3t63g40mm20n01	6280	4.00	–2.0	6
d3t63g40mm10n01	6260	4.00	–1.0	6
d3t63g40mm30n02	6240	4.00	–3.0	12
d3t63g40mm20n02	6250	4.00	–2.0	12
d3t63g40mm10n02	6250	4.00	–1.0	12

Table 1. Parameters of 3D models. The model a was used in the analysis of SDSS J1349-0229. We interpolated between the corrections from the models b for SDSS J0912+0216. #OB denotes the number of opacity bins - see discussion for details.

Table 2. 3D and 1D abundances expressed with respect to solar abundances of log(ϵ) = 8.50, 7.86, and 8.76 for C, N and O, respectively.

	SDSS J1349-0229		SDSS J0912+0216	
Element	$[X/Fe]_{1D}$	$[X/Fe]_{3D}$	$[X/Fe]_{1D}$	$[X/Fe]_{3D}$
CH	2.82	2.09	2.17	1.67
C_2	3.16	1.72		
C I NLTE	2.42	2.51	1.38	1.44
NH	1.60	0.67	1.75	1.07
OH	1.88	1.69		
O I NLTE	1.63	1.69		

Discussion

The sensitivity of the molecular lines to temperature is clear from the significant 3D corrections. In Figure 1 we have plotted the temperature distributions for the models. The ranges of depth of formation of the lines used in the analysis are overplotted for comparison. The different depth of formation of the C_2 and CH lines in the 1D and 3D models explains why in 1D we derive a larger C abundance from the C_2 lines than from the CH lines, while in 3D the reverse is true. The C_2 lines are formed much higher up in the atmosphere compared to the CH lines, and this tendency is much larger in the 3D model than in the 1D. The 3D models on the other hand do not achieve a better consistency between CH and C_2 lines. The C I lines are quite insensitive to 3D effects. Neither in 3D nor in 1D we achieve consistent results between molecular lines and C I.

In the hopes to shed light on the discrepancy between the carbon abundance indicators, we use our best indicator, C I as a reference and explore the influence of the 3D model properties on the molecular abundance determination. In particular, we explore the effect of increasing the number of opacity bins in the opacity groups from 6 bins to 12 bins. The models presented here are listed in Table 1. The new abundance obtained for SDSS J1349-0229 are listed in this Table:

	CH	C_2	C I NLTE	NH	OH	O I NLTE
6 bin $[X/Fe]_{3D}$	2.09	1.72	2.51	0.67	1.69	1.69
12 bin $[X/Fe]_{3D}$	2.22	1.99	2.50	0.87	1.69	1.68

The temperature distribution of the 12 bin model is shown in Figure 1 below the 6 bin model. The different binning scheme results in a decrease of the overcooling, thus lowering the 3D corrections of the molecules formed higher in the atmosphere. The corrections are displayed as a function of metallicity in Figure 2. The atomic lines, formed deeper in the atmosphere are unaffected. The 12 bin models give a better agreement between the CH the C_2 lines and both molecular features appear to be in better agreement with the C I. Although these results appear encouraging, the formation region, is so external and low density, that the validity of LTE for molecule formation and levels population should be questioned.

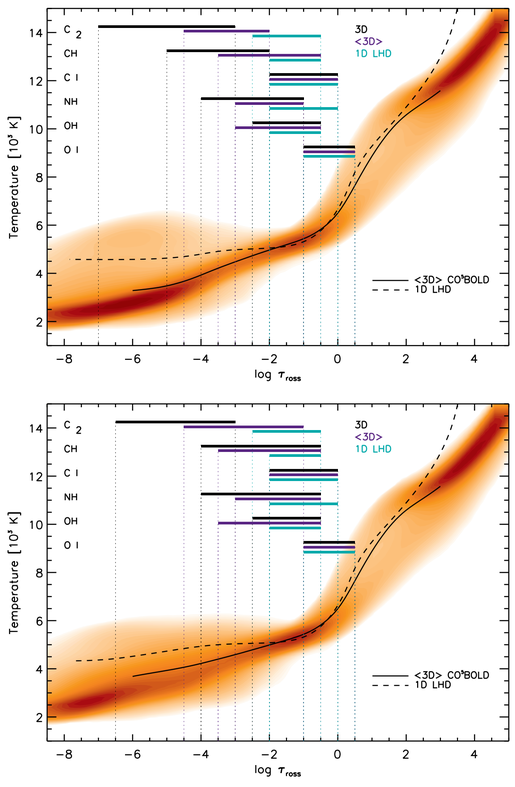

Figure 1. The temperature structures of the 3D 6 bin model d3t63g40mm30n01 (top) and 12 bin model d3t63g40mm30n02 (bottom) are plotted as a function of optical depth along with the average 3D and corresponding 1D temperature structures. Overplotted on the figure are the ranges of depth of formation of the C_2, CH, C I, NH, OH and O I spectral lines used in the analysis.

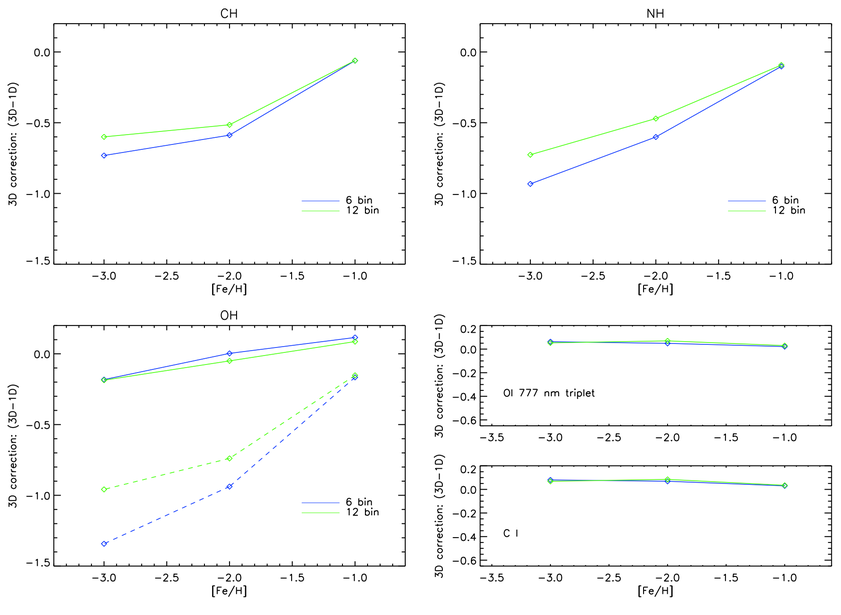

Figure 2. 3D corrections as a function of metallicity for CH, OH, NH, O I and C I. The 6 bin models are plotted in blue, while the 12 bin models are plotted in green. The OH correction have been calculated assuming a typical CEMP composition: an enhanced carbon-to-oxygen ratio of +1.0. Overplotted as dashed lines are the corrections using scaled solar abundances.

References

Asplund M., Nordlund A., Trampedach R., Stein R. 1999, A&A, 346, L17
Behara N.T., et al., 2009, in preparation
Bonifacio P., Molaro P., Beers T.C., Vladilo G. 1998, A&A, 332, 672
Caffau E., Ludwig H.-G. 2007, A&A, 467, L11
Freytag B., Steffen M., Dorch B., 2002, AN, 323, 213
Goldman A., & Gillis J. R., 1981, JQSRT, 25, 111
González Hernández J.I., et al. 2008, A&A, 480, 233
Kurucz R.L. 2005, http://kurucz.harvard.edu
Wedemeyer S., et al. 2004, A&A 414, 1121